Published OnlineFirst July 2, 2019; DOI: 10.1158/1541-7786.MCR-19-0197

Molecular Cancer Research

Ubiquitin-Specific Protease 3 Promotes Glioblastoma Cell Invasion and Epithelial–Mesenchymal Transition via Stabilizing Snail

Ligang Fan[1], Zhengxin Chen[1], Xiaoting Wu[2], Xiaomin Cai[1], Shuang Feng[1], Jiacheng Lu[1], Huibo Wang[1], and Ning Liu[1]

Abstract

Epithelial–mesenchymal transition (EMT) represents one of the most important events in the invasion of glioblastomas (GBM); therefore, better understanding of mechanisms that govern EMT is crucial for the treatment of GBMs. In this study, we report that the deubiquitinase ubiquitin-specific protease 3 (USP3) is significantly upregulated in GBMs and correlates with a shorter median overall and relapse-free survival. Silencing of USP3 attenuates the migration and invasion abilities of GBM cells *in vitro* and tumor growth in an orthotopic xenograft mouse model. Mechanistically, we identify USP3 as a bona fide deubiquitinase for Snail, a master transcription factor that promotes EMT, in GBM cells. USP3 interacts directly with Snail and stabilizes Snail via deubiquitination. Ectopic expression of Snail could largely rescue the inhibitory effects of USP3 depletion on migration, invasion, and tumor growth of GBM cells. In addition, we found that USP3 strongly correlates with Snail expression in primary human GBM samples. Overall, our findings reveal a critical USP3–Snail signaling axis in EMT and invasion, and provide an effective therapeutic approach against GBM.

Implications: Our study establishes USP3-mediated Snail stabilization as an important mechanism underlying GBM invasion and progression, and provides a rationale for potential therapeutic interventions in the treatment of GBM.

Introduction

High-grade gliomas (HGG), in particular glioblastoma multiforme (GBM), are the most common and lethal primary malignant brain tumor in adults (1, 2). Despite recent advances in multimodal therapies, including surgical resection followed by radiation and chemotherapy, the prognosis for patients with GBM remains gloomy (3, 4). The median overall survival (OS) is about 12–15 months after diagnosis and the 5-year survival rates are <9.8% following a standard care (5, 6). A major obstacle to cure this devastating disease is attributed to its highly invasive nature (7, 8). Thus, understanding the mechanism underlying GBM invasiveness is critical for developing more effective strategies for treating GBM.

Epithelial–mesenchymal transition (EMT) is a complex process, in which epithelial cells acquire the characteristics of invasive mesenchymal cells (9), which has been implicated in the formation of many tissues and organs during embryonic development, as well as tumor invasion and progression. The EMT program is triggered by the activation of core transcription factors, including Snail1/2, ZEB1/2, and Twist1/2 (9). Numerous studies have suggested that these EMT-inducing transcription factors are aberrantly expressed in multiple types of tumors and are known to favor the invasive process (10, 11).

Deubiquitinating enzymes (DUB) are a large group of proteases that remove ubiquitin chains from substrate proteins. So far, there are about more than 100 putative DUBs in the human proteome including five families: ubiquitin-specific proteases (USP), ubiquitin carboxy-terminal hydrolases, ovarian tumor proteases, Machado-Joseph disease proteases, and JAB1/MPN/Mov34 metalloenzymes (12). USP family represents the largest subclass of DUBs with about 60 members. USP3, a member of the USP superfamily, plays a pivotal role in regulating diverse biological processes. For instance, USP3 interacts with and deubiquitylates CHK1, thereby suppressing cell survival under stress and genome stability (13). USP3 deubiquitylates and stabilizes p53 and promotes normal cell transformation (14). USP3 inhibits RIG-I signaling and antiviral immunity by binding RIG-I and deubiquitylating K63-linked polyubiquitin chains on RIG-I (15). USP3 also deubiquitylates H2A and γH2AX at lysine 13 and 15 via negatively regulating DNA damage response (16). More recently, USP3 has been found to be significantly upregulated in gastric cancer (17). Nevertheless, the role of USP3 in other types of cancers remains undetermined.

In this study, we showed that USP3 was markedly overexpressed in human GBM specimens and cell lines. Depletion of USP3 dramatically inhibited migration, invasion, and tumor growth by blocking EMT in GBM cells. Furthermore, we identified

[1]Department of Neurosurgery, First Affiliated Hospital of Nanjing Medical University, Nanjing, Jiangsu Province, China. [2]Department of Cardiology, First Affiliated Hospital of Nanjing Medical University, Nanjing, Jiangsu Province, China.

Note: Supplementary data for this article are available at Molecular Cancer Research Online (http://mcr.aacrjournals.org/).

L. Fan and Z. Chen contributed equally to this article.

Corresponding Authors: Ning Liu, First Affiliated Hospital of Nanjing Medical University, Nanjing 210029, Jiangsu, China. Phone: 8625-6830-3152; Fax: 8625-6830-6772; E-mail: liuning853@126.com; and Huibo Wang, hbwang@njmu.edu.cn

Mol Cancer Res 2019;XX:XX–XX

doi: 10.1158/1541-7786.MCR-19-0197

Published OnlineFirst July 2, 2019; DOI: 10.1158/1541-7786.MCR-19-0197

USP3 as a *bona fide* DUB that regulates EMT-inducing transcription factor Snail polyubiquitylation and stabilization, which thereby promotes EMT and invasion in GBM.

Materials and Methods

Cell culture and antibodies

The human glioma cell lines (Hs683 and SW1783), the human embryonic kidney cell line (293T), and human GBM cell lines U87MG, U118, and LN229 were purchased from the ATCC. The human GBM cell lines U251 and T98G were obtained from RIKEN BioResource Center. These cell lines were then grown in DMEM supplemented with 10% FBS. Normal human astrocytes (NHA) were obtained from Lonza and cultured in the provided astrocyte growth media supplemented with recombinant human Epidermal Growth Factor (rhEGF), insulin, ascorbic acid, GA-1000, L-glutamine, and 5% FBS. All the cells used in this study were authenticated by serial short tandem repeat profiling and tested for *Mycoplasma* contamination. Antibodies against USP3, E-cadherin, N-cadherin, Vimentin, Fibronectin, Snail, ZEB1, ZEB2, Twist1, Myc tag, HA tag, and Flag tag were purchased from Abcam. β-actin was purchased from Cell Signaling Technology.

Human tissue samples

Glioma specimens (grade I–II = 2, grade III = 3, and grade IV = 6) and normal brain tissues (NBT; $n = 2$) were obtained from The First Affiliated Hospital of Nanjing Medical University (Nanjing, China). One hundred and thirty-two GBM patients were obtained from Department of Neurosurgery, the Second and Fourth Affiliated Hospitals of Harbin Medical University (Harbin, China). The Research Ethics Committee of Nanjing Medical University and Harbin Medical University approved the use of GBMs and NBTs, and the procedures were performed in accordance with the approved guidelines. Permissions were obtained from participants, and patients granted informed consent.

IHC

IHC was performed to detect the expression of USP3 or Snail in human glioma specimens or NBTs as described previously (18).

Stable cell establishment

U87MG and T98G cell lines stably expressing USP3-specific short hairpin RNA (USP3-shRNA) or scrambled shRNA control were constructed using a lentiviral shRNA technique. Oligonucleotides were constructed in hCMV lentiviral RNAi vector (Dharmacon). U87MG or T98G was transduced with serial dilutions of lentiviral supernatant and selected for using 5 mg/mL puromycin for 3 to 4 weeks. The human USP3 shRNA targeting sequences are listed as follows. The targeting sequence for USP3-shRNA#1 was 5′-GTAATGTCCAGAACCAACC-3′; the targeting sequence for USP3-shRNA#2 was 5′-AGTTTATCCGATCCAGCTT-3′; the targeting sequence for USP3-shRNA#3 was 5′-AATGGATCAAACTTTCTAG-3′; the targeting sequence for USP3-shRNA#4 was 5′-GGCTCTAGTAAGTAGCATT-3′; the targeting sequence for USP3-shRNA#1(targeting 3′UTR; untranslated region) was 5′-TTTAGAGTCAACCTGATGT-3′; and the targeting sequence for USP3-shRNA#2(targeting 3′UTR) was 5′-AGCAAATCAAAACATCTGC-3′;

Wound-healing assays

U87MG or T98G cells were seeded in 24-well plates containing coverslips. The uniformly covered monolayer cells were scratched by the tip of a 20 mL plastic pipette. The cell residue on the coverslip was rinsed with PBS. The scratched area was photographed with a microscope (Leica). The wound-healing effect of U87MG or T98G cells was calculated into a migration index. Experiments were carried out at least triplicate.

Transwell and 3D collagen spheroid invasion assays

Transwell invasion assay was performed using 24-well BD Matrigel Invasion Chambers (BD Biosciences) as our previous study described (19).

For 3D collagen spheroid invasion assay, glioma cells planked in the 3D culture qualified 96-well spheroid formation plate were incubated at 37°C in a tissue culture incubator for 72 hours to promote spheroid formation. Plate with invasion matrix per well was transferred to a tissue culture incubator set at 37°C for 1 hour to promote gel formation. Spheroids in every well were added to cell culture medium containing collagen I (Invitrogen), 10% FBS, and 10% $NaHCO_3$. The spheroids were photographed in each well every 24 hours using a JuLI Image Viewer (NanoEnTek).

Cell extraction and Western blotting

Cellular proteins were lysed by RIPA buffer containing protease inhibitors (Roche), and equal amount of proteins were electrotransfered onto a polyvinylidene difluoride membrane (Millipore). Protein was incubated by the primary and secondary antibodies and then detected with the enhanced chemiluminescence methods.

RNA extraction and qPCR analysis

RNA was extracted using TRizol (Invitrogen). First strand cDNA was synthesized using the PrimeScript RT Master Mix (TaKaRa). Real-time PCR was performed using SYBR Green (Applied Biosystems). The forward and reverse PCR primers for Snail were 5′-ACCCCACATCCTTCTCACTG-3′ and 5′-CAGGCAGAGGACACAGAACC-3′; the primers for E-cadherin were 5′-CACCCTGGCTTTGACGCCGA-3′ and 5′-AAAATTCACTCTGCCCAGGACGCG-3′; the primers for N-cadherin were 5′- CGCCATCCAGACCGACCCAA-3′ and 5′- GTCGATTGGTTTGACCACGGTGAC-3′; the primers for Vimentin were 5′-GACGCCATCAACACCGAGTT-3′ and 5′-CTTTGTCGTTGGTTAGCTGGT-3′; and the primers for Fibronectin were 5′-CGGTGGCTGTCAGTCAAAG-3′ and 5′-AAACCTCGGCTTCCTCCATAA-3′; GAPDH mRNA was also amplified in the same PCR reactions as an internal control using the primers 5′-TGTAGTTGAGGTCAATGAAGGG-3′ and 5′-ACATCGCTCAGACACCATG-3′.

Immunoprecipitation and ubiquitylation assay

Cells were lysed using RIPA lysis buffer containing protease inhibitor. Total protein lysate was immunoprecipitated with the indicated primary antibody on protein A/G beads (Santa Cruz Biotechnology) at 4°C for overnight. The protein A/G beads were washed by prechilled washing buffer and then boiled for 10 minutes in 2 × SDS loading buffer. Western blotting was performed to evaluate immunoprecipitated protein complexes. To test Snail ubiquitylation, the lysis buffer was added with N-ethylmaleimide (Sigma-Aldrich).

Published OnlineFirst July 2, 2019; DOI: 10.1158/1541-7786.MCR-19-0197

Intracranial xenograft tumor models

Experiments were performed using 4- to 5-week-old NOD/SCID mice. For intracranial xenograft studies, 1.5×10^5 luciferase-encoding U87MG cells with designated modification were intracranially injected into the striatum of immunocompromised mice using a stereotactic device (coordinates: 2 mm anterior, 2 mm lateral, 3 mm depth from the dura). Tumor progression was monitored using *in vivo* bioluminescence imaging. The mice were humanely euthanized 5 to 10 weeks after implantation, and their brains were removed, paraffin embedded, stained with hematoxylin and eosin (H & E) to ascertain the presence of tumor. All animal experiments were conducted with the approval of Institutional Animal Care and Use Committee of Nanjing Medical University and in conformity with the Guide for the Care and Use of Laboratory Animals (National Academies Press, 2011).

Statistical analysis

All data were analyzed in biological triplicate with SEM subjected to two-tail student *t* tests for two group comparisons or one-way ANOVA for three group comparisons. Kaplan–Meier survival curves were drawn by GraphPad Prism 7 software. For all statistical tests, $P < 0.05$ was considered to be statistically significant.

Results

USP3 is upregulated in GBM tissues and cell lines

We initially analyzed the expression of USP3 using gene expression profiling interactive analysis (GEPIA) (http://gepia.cancer-pku.cn/). As shown in Fig. 1A, USP3 mRNA levels were found to be significantly upregulated in GBM specimens ($n = 163$) as compared with NBTs ($n = 207$). We then examined USP3 expression in different grades of glioma specimens (grade I–II 2; grade III 3; and grade IV 6) and two NBTs. We found that USP3 was weakly expressed in NBTs, but was highly expressed in glioma specimens, especially GBMs (Fig. 1B and C). Moreover, we assessed the protein levels of USP3 in five GBM cell lines (T98G, U251, U87MG, U118, and LN229), two human glioma cell lines Hs683 and SW1783 (grade III), and NHAs. The results showed that USP3 protein levels were markedly higher in all five tested GBM cell lines than those in Hs683 and SW1783 as well as NHAs (Fig. 1D). Together, these data suggest USP3 is aberrantly expressed in GBM tissues and cell lines.

USP3 depletion inhibits invasion, migration, and tumor growth of GBM cells by blocking EMT

A recent study has reported that USP3 is associated with invasion and migration of gastric cancer cells (17). Accordingly, we wondered whether USP3 is involved in regulating invasion and migration of GBM cells. To test this, we knocked down USP3 expression in U87MG and T98G cells using four independent green fluorescent protein-encoding shRNAs. Western blot analysis confirmed that USP3 protein levels were significantly reduced in cells transduced with USP3 shRNAs compared with those transduced with control shRNA (Fig. 2A). We then performed the wound-healing assay and observed that silencing of USP3 markedly suppressed the migration of U87MG and T98G cells (Fig. 2B and C). Moreover, transwell-Matrigel invasion assay and 3D collagen spheroid invasion assay were carried out, respectively. USP3 knockdown remarkably inhibited the invasion of U87MG and T98G cells in transwell with Matrigel (Fig. 2D and E). 3D collagen spheroid invasion assay showed that the area covered by invading cells was decreased by 2.8-fold in U87MG and by 3.8-fold in T98G transduced with USP3 shRNAs (Fig. 2F and G). The invaded distance was decreased by 2.1-fold in U87MG and by 2.4-fold in T98G transduced with USP3 shRNAs (Fig. 2F and H). We then evaluated the effect of USP3 depletion on tumorigenic potential of GBM *in vivo*, equal amount of luciferase-encoding U87MG cells transduced with shCtrl or shUSP3 were intracranially injected

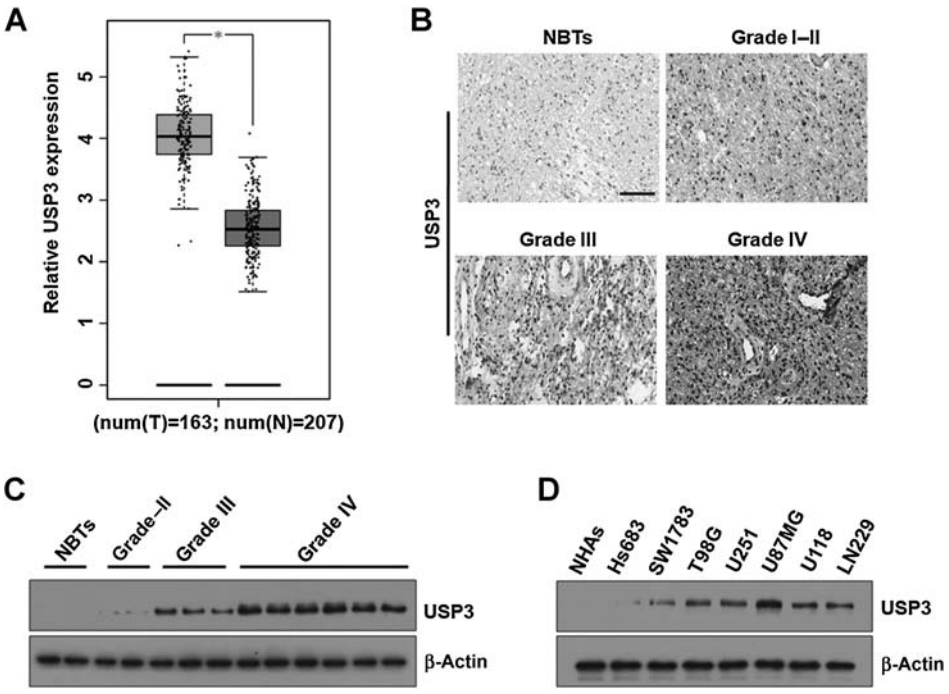

Figure 1.
USP3 is upregulated in GBM tissues and cell lines. **A,** Expression of USP3 analysis using GEPIA (*, $P < 0.05$). **B,** IHC staining analysis of USP3 protein levels in normal brain and glioma tissues (grade I–IV). **C,** USP3 protein levels were analyzed by Western blot analysis in NBTs and different grades of glioma specimens. β-actin was used as loading control. **D,** Western blot analysis of USP3 protein levels in NHAs and the established glioma cell lines. β-actin was used as loading control.

Published OnlineFirst July 2, 2019; DOI: 10.1158/1541-7786.MCR-19-0197

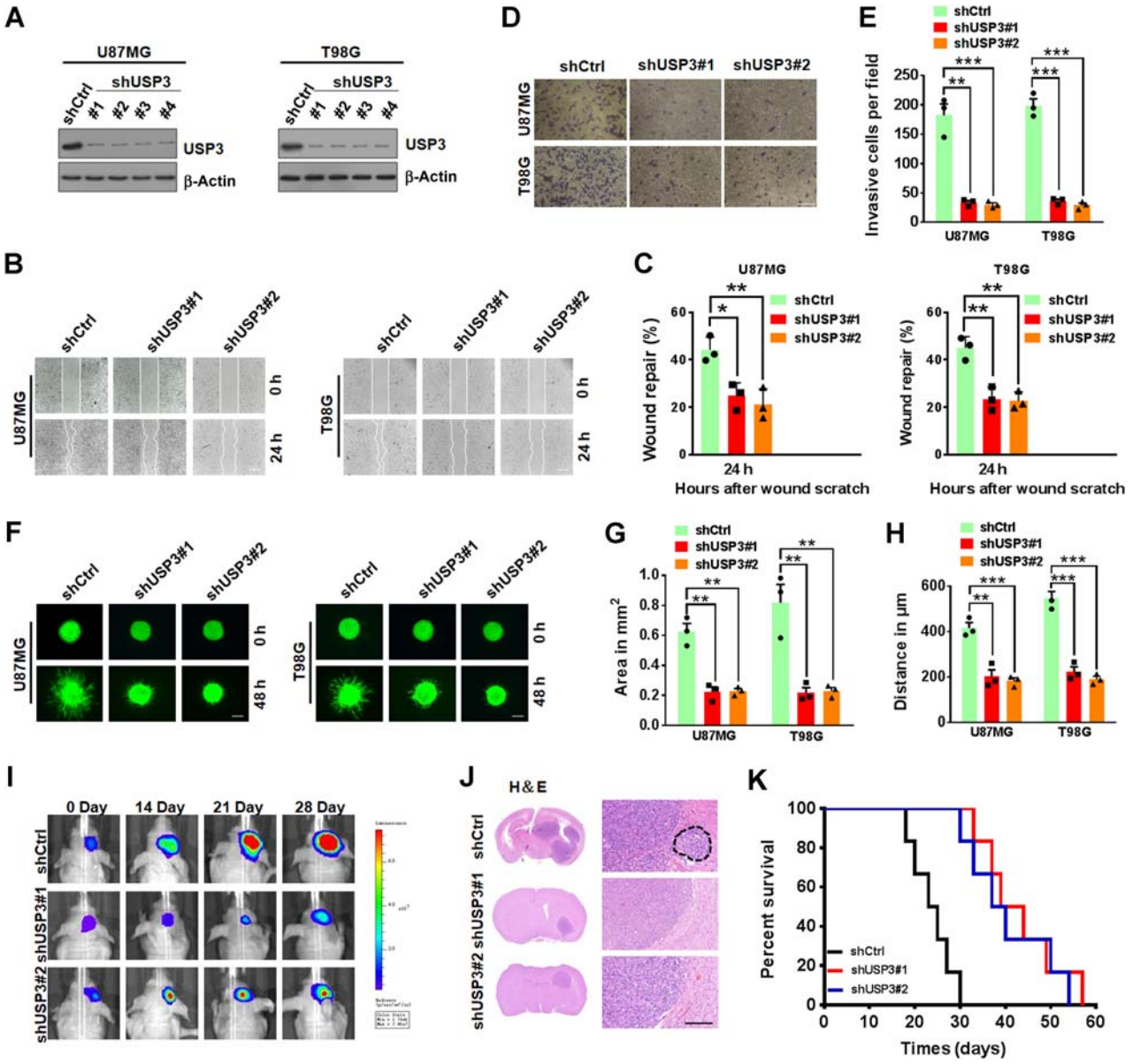

Figure 2.

USP3 depletion inhibits invasion, migration, and tumor growth of GBM cells by blocking EMT. **A,** Western blot analysis of USP3 protein levels in U87MG and T98G cells transduced with USP3 shRNAs (shUSP3) or control shRNA (shCtrl). β-actin was used as loading control. **B,** Representative images of wound-healing assay using U87MG and T98G cells stably transduced with USP3 shRNAs or control shRNA. **C,** The quantification of wound-healing assay is shown; *, $P < 0.05$; **, $P < 0.01$. **D,** Representative images of transwell invasion assay using U87MG and T98G cells stably transduced with USP3 shRNAs or control shRNA. **E,** The quantification of transwell invasion assay is shown; **, $P < 0.01$; ***, $P < 0.001$. **F,** Representative images of 3D collagen spheroid invasion assay using U87MG and T98G cells stably transduced with USP3 shRNAs or control shRNA; scale bar, 200 μm. **G** and **H,** The quantification of 3D collagen spheroid invasion assay is shown; **, $P < 0.01$; ***, $P < 0.001$. **I,** Representative bioluminescent images of intracranial GBM xenografts derived from U87MG cells with indicated modifications. Quantification of bioluminescent images is shown on the right. Colored scale bars represent photons/s/cm^2/steradian. **J,** H & E–stained brain sections from mice intracranially implanted with U87MG cells with indicated modifications. The dotted circle indicates invasive tumors. **K,** Kaplan–Meier survival curves of mice intracranially injected with U87MG cells with indicated modifications; $P < 0.001$.

into immunodeficient mice. Compared with the control group, mice implanted with USP3-depleted U87MG cells exhibited extended survival with a lower rate of tumor formation and decreased invasive activity (Fig. 2I–K).

It is known that EMT is one of the key factors for tumor cells to obtain their ability of migration and invasion, which is mediated by a core set of key transcription factors. Thus, we asked whether USP3 could affect the EMT process. To that end, we examined the expression of EMT-associated molecules, including epithelial marker E-cadherin, as well as mesenchymal markers N-cadherin, vimentin, and fibronectin after USP3 depletion. We found that USP3-depleted U87MG and T98G

Published OnlineFirst July 2, 2019; DOI: 10.1158/1541-7786.MCR-19-0197

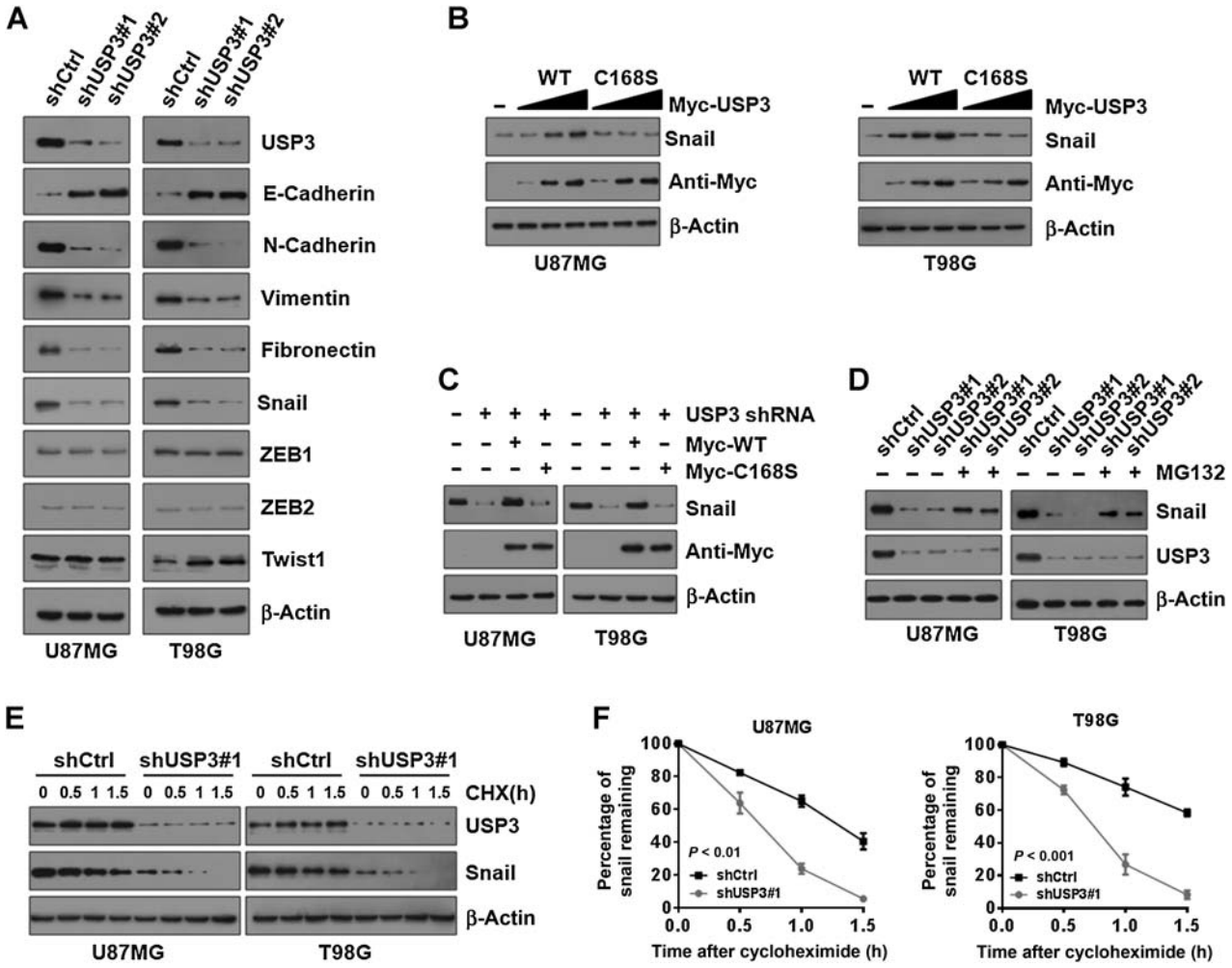

Figure 3.

USP3 maintains the stability of Snail. **A,** U87MG and T98G cells were stably transduced with two independent shRNAs targeting USP3 (shUSP3) or control shRNA (shCtrl). Western blotting was performed with the indicated antibodies. β-actin was used as loading control. **B,** Increasing amounts of USP3 WT or C168S were transfected into U87MG and T98G cells and Snail protein levels were detected. β-actin served as loading control. **C,** USP3 WT or C168S was transfected into U87MG and T98G cells together with shRNA targeting USP3 3′UTR. Snail protein levels were measured. β-actin served as loading control. **D,** U87MG and T98G cells transduced with two specific USP3 shRNAs were treated with or without the proteasome inhibitor MG132 (20 μmol/L, 8 hours), then Snail and USP3 proteins were analyzed. β-actin served as loading control. **E,** Treated U87MG and T98G stably transduced the indicated shRNA cells with cycloheximide (10 μg/mL), half-life of Snail was analyzed. β-actin served as loading control. **F,** Quantification of Snail levels relative to β-actin is shown.

cells showed a significant decrease in N-cadherin, vimentin, and fibronectin mRNA and protein levels, and an increase in E-cadherin levels compared with control cells (Fig. 3A; Supplementary Fig. S1A). Moreover, we assessed the expression of several core EMT-inducing transcription factors, including Snail, ZEB1, ZEB2, and Twist1. Intriguingly, reduced protein expression of Snail, but not other EMT-inducing transcription factors, was observed in USP3-depleted U87MG and T98G cells when compared with control cells (Fig. 3A). However, both Snail (Supplementary Fig. S1B) and other EMT-inducing transcription factors' mRNA levels were not affected by USP3 silencing (data not shown).

USP3 maintains the stability of Snail

On the basis of the above findings, we hypothesized that the reduction of Snail protein levels caused by USP3 depletion might possibly result from Snail protein degradation. To test this, we constructed the Myc-tagged USP3 wild-type (WT) and catalytically inactive mutant C168S plasmids and transfected them into U87MG and T98G cells. We found that ectopic expression of WT USP3, but not C168S USP3, which lost its DUB activity, resulted in Snail protein elevation in a dose-dependent manner in U87MG and T98G cells (Fig. 3B). Conversely, knockdown of USP3 significantly reduced Snail protein levels, which could be reversed by WT but not C168S USP3 or addition of the proteasome inhibitor MG132 in two GBM cells (Fig. 3C and D). Furthermore, we treated U87MG and T98G cells with the protein synthesis inhibitor cycloheximide and analyzed Snail protein degradation rates. As shown in Fig. 3E and F, the degradation rate of Snail was profoundly accelerated when endogenous USP3 was depleted. Together, these findings suggest that USP3 stabilizes Snail in GBM cells.

Published OnlineFirst July 2, 2019; DOI: 10.1158/1541-7786.MCR-19-0197

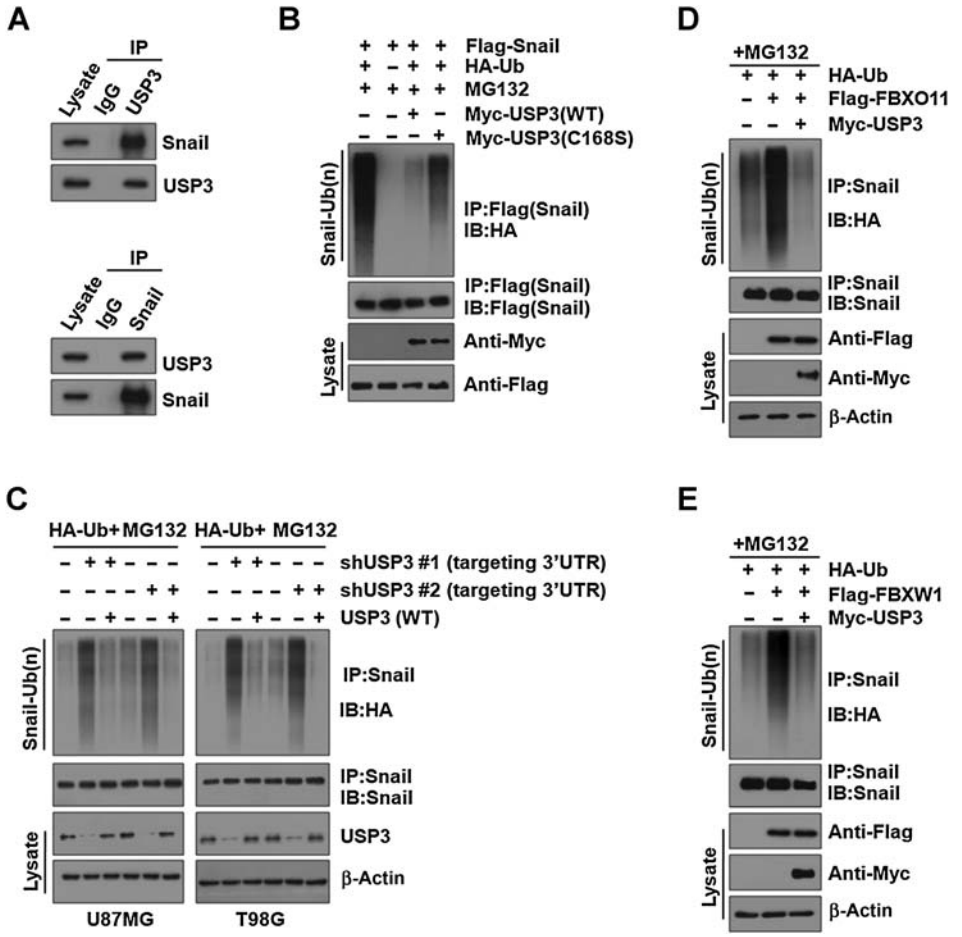

Figure 4.
USP3 stabilizes Snail1 through deubiquitination. **A,** U87MG cells lysates were subject to immunoprecipitation (IP) with control IgG, anti-USP3, or Snail antibodies. The immunoprecipitates were then blotted (IB). **B,** Ubiquitylated Snail was purified from MG132-treated HEK293T cells expressing Flag-Snail and then incubated with purified Myc-tagged WT USP3 or C168S-USP3 in an *in vitro* deubiquitylation assay. The polyubiquitylated state of Snail was examined by Western blotting using HA antibody. Immunopurified Snail and USP3 used in this assay were analyzed using Flag and Myc antibodies, respectively. **C,** U87MG and T98G cells transduced with two targeting USP3 3′UTR shRNAs were transfected with or without USP3 WT, and then the polyubiquitylated state of Snail was tested. **D** and **E,** Snail ubiquitylation was analyzed in U87MG cells transfected with E3 FBXO11 (**D**) or FBXW1 (**E**) together with USP3 or not.

USP3 stabilizes Snail1 through deubiquitination

To further confirm the association between USP3 and Snail, we carried out reciprocal coimmunoprecipitation experiments with antibody against USP3 or Snail. As shown in Fig. 4A, endogenous USP3 and Snail were immunoprecipitated from U87MG cells and the presence of endogenous Snail and USP3 were detected. Moreover, we transduced Myc-tagged WT or C168S-USP3 into HEK293T cells and found that WT, but not C168S USP3, specifically removed Snail ubiquitylation (Fig. 4B). Furthermore, depletion of USP3 by two independent shRNAs increased Snail polyubiquitylation in U87MG and T98G cells, which could be restored by WT-USP3 (Fig. 4C). Recent studies have demonstrated that Snail can be ubiquitylated and degraded by the E3 ligases, including FBXO11 (20) and FBXW1 (21). As such, we interrogated whether USP3 could counteract the actions of these two E3 ligases. Indeed, overexpression of USP3 largely rescued FBXO11- or FBXW1-induced Snail polyubiquitylation (Fig. 4D and E). Collectively, these results indicate that USP3 is a specific DUB targeting Snail protein for stabilization.

Snail is required for USP3-mediated invasion, migration, and tumor growth of GBM cells

To examine the role of Snail in USP3-induced GBM cells invasion and migration, we ectopically transduced Snail or empty vector control into U87MG and T98G cells, in which endogenous USP3 had been stably depleted (Fig. 5A). We found that the suppressive effect of USP3 depletion on invasion and migration of U87MG and T98G cells could be largely rescued by Snail (Fig. 5B–H). We next performed the *in vivo* experiment and found that Snail was able to restore the loss of tumorigenic capacity caused by silencing of USP3 (Fig. 5I–K). These results demonstrate that Snail is critical for USP3-mediated invasion, migration, and tumor growth of GBM cells. Our findings suggest the important role of USP3/Snail signaling axis in mediating the invasive and tumorigenic properties of GBM cells.

USP3 is positively correlated with Snail protein expression and is associated with poor survival of human GBMs

To assess the clinical relevance of our findings, we carried out IHC analysis of USP3 and Snail using a tissue microarray containing 132 patients with GBM. A highly significant positive correlation between USP3 and Snail was found in these GBM specimens. Tumors with high USP3 levels express high Snail levels, whereas tumors with low USP3 levels display low Snail levels (Fig. 6A and B). Next, we tested whether USP3 expression was associated with the prognosis of patients with GBM. Kaplan–Meier survival analysis revealed that patients with high expression of USP3 ($n = 66$) exhibited much worse OS and disease-free survival (DFS) than those with low expression of USP3 ($n = 66$; Fig. 6C and D). In agreement with our results, analysis of USP3 expression using the TCGA database

Published OnlineFirst July 2, 2019; DOI: 10.1158/1541-7786.MCR-19-0197

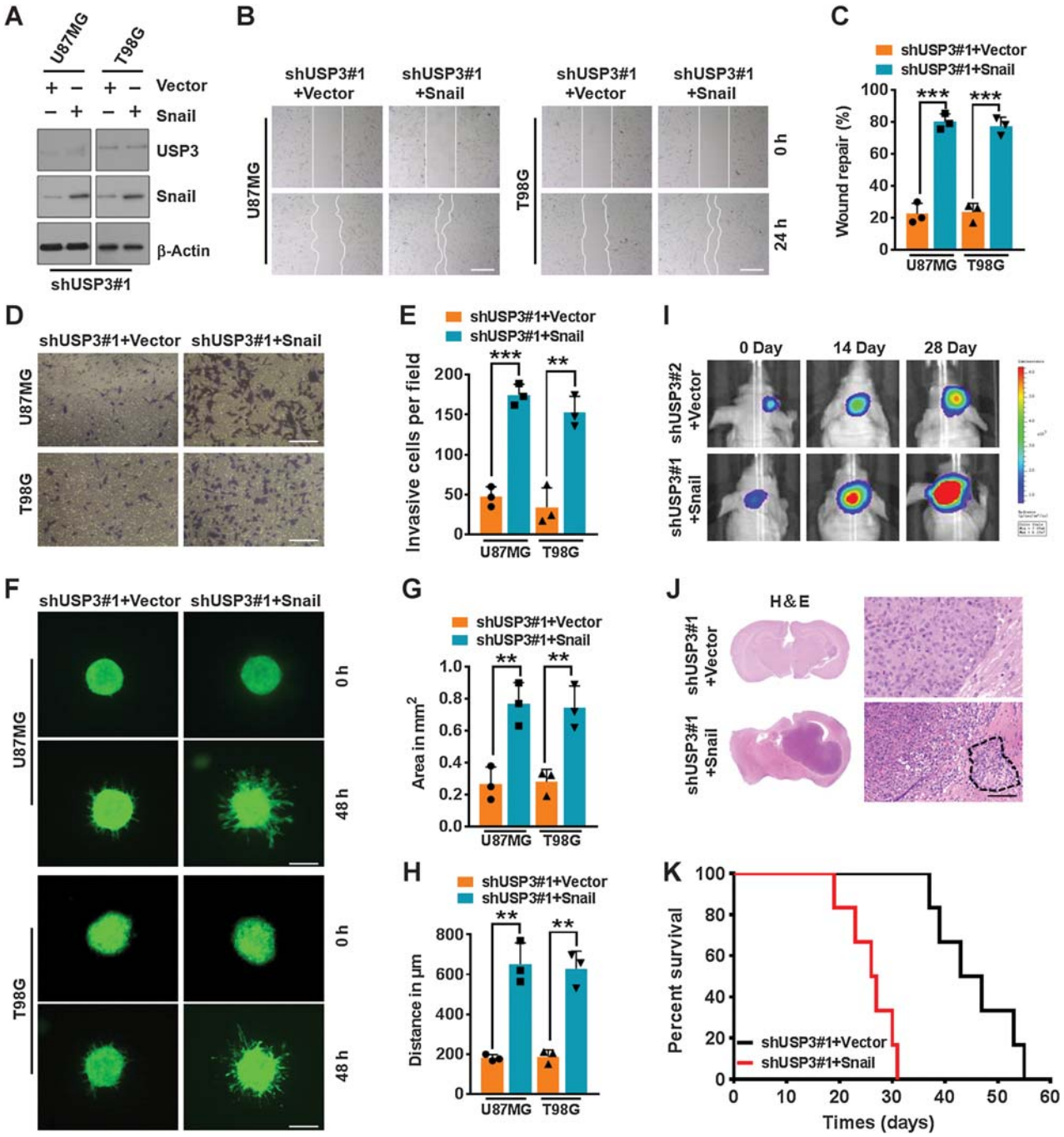

Figure 5.

Snail is required for USP3-mediated invasion, migration, and tumor growth of GBM cells. **A,** Western blot analysis of USP3 protein levels in U87MG and T98G cells transduced with control shRNA or USP3 shRNAs (shUSP3), reconstituted with vector control or Snail. β-actin was used as loading control. **B,** Representative images of wound-healing assay using U87MG and T98G cells with indicated modifications. **C,** The quantification of wound-healing assay is shown; ***, $P < 0.001$. **D,** Representative images of transwell invasion assay using U87MG and T98G cells with indicated modifications. **E,** The quantification of transwell invasion assay is shown; **, $P < 0.01$; ***, $P < 0.001$. **F,** Representative images of 3D collagen spheroid invasion assay using U87MG and T98G cells with indicated modifications. **G** and **H,** The quantification of 3D collagen spheroid invasion assay is shown; **, $P < 0.01$. **I,** Representative bioluminescent images of intracranial GBM xenografts derived from U87MG cells with indicated modifications. Quantification of bioluminescent images is shown on the right. Colored scale bars, photons/s/cm^2/steradian. **J,** H & E–stained brain sections from mice intracranially implanted with U87MG cells with indicated modifications. The dotted circle indicates invasive tumors. **K,** Kaplan–Meier survival curves of mice intracranially injected with U87MG cells with indicated modifications; $P < 0.0001$.

Published OnlineFirst July 2, 2019; DOI: 10.1158/1541-7786.MCR-19-0197

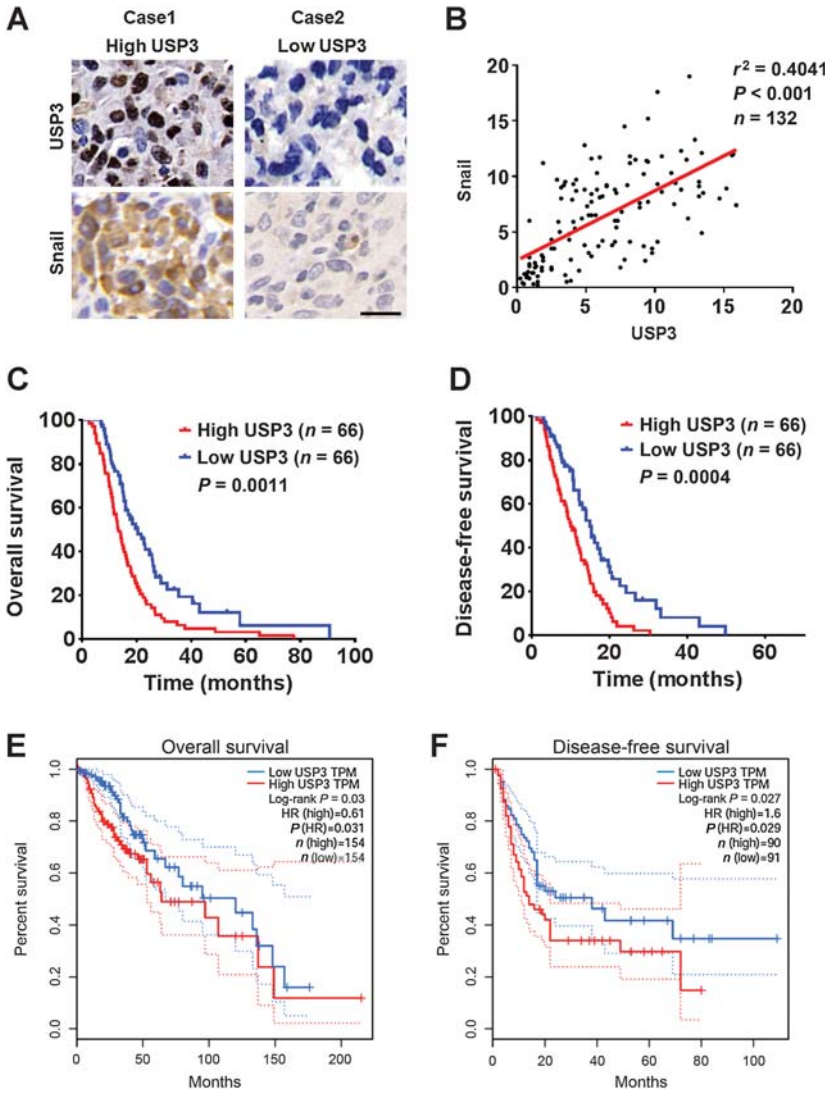

Figure 6.

USP3 is positively correlated with Snail protein expression and is associated with poor survival of human GBMs. **A,** IHC staining of USP3 and Snail in human GBM tissues. Representative images of IHC staining from the same tumor samples are shown. **B,** Spearman correlation analysis between USP3 and Snail protein levels in GBM specimens. Kaplan–Meier curves of OS (**C**) or DFS (**D**) for patients with high ($n = 66$) or low ($n = 66$) USP3 expression. Kaplan–Meier curves show the OS (**E**) or DFS (**F**) of patients with high or low expression of USP3 using the TCGA database.

showed that high expression of USP3 correlated with poor OS and DFS in patients with GBM (Fig. 6E and F). Taken together, these data suggest that USP3 positively correlates with Snail and acts as a potential prognostic indicator for patients with GBM.

Discussion

EMT, originally identified as a crucial process that regulates various aspects of embryonic development and tissue homeostasis, is now recognized as a key regulator of cancer progression by facilitating tumor cell invasion and dissemination (22–25). Therefore, targeting EMT represents an important therapeutic strategy for cancer treatment. In this study, we found that USP3 is markedly overexpressed in GBM specimens and contributes to GBM cell migration and invasion via promoting EMT by stabilizing Snail. We demonstrated that USP3 directly interacts with and deubiquitylates Snail, which could counteract FBXO11- or FBXW1-induced Snail polyubiquitylation, leading to the enhanced invasive and tumorigenic properties in GBM.

Previous studies have unveiled the diverse functions of USP3 in regulating cellular biological process (13, 14, 16). However, little is known about the role of USP3 in cancer biology. Notably, a recent study performed by Fang and colleagues showed that USP3 is highly expressed in gastric cancer and could promote the migration and invasion of gastric cancer cells (17). Intriguingly, another study showed that USP3 plays a role as a tumor suppressor in colorectal cancer, and the loss of USP3 is associated with distal metastasis and a dismal prognosis (26). These findings suggest that USP3 might have context-dependent oncogenic or tumor suppressive activities in human cancers. In this study, we identified USP3 as an oncoprotein that could facilitate invasion, migration, and tumor growth in GBM. Knockdown of USP3 by shRNA interference dramatically inhibited the migration and invasion of GBM cells. More importantly, *in vivo* experiments showed that depletion of USP3 markedly repressed tumor growth of U87MG-derived intracranial xenografts. These results suggest that USP3 may be an attractive target for therapeutic intervention in GBM. Although there are currently no selective USP3 antagonists available for clinical use, our results provide

Published OnlineFirst July 2, 2019; DOI: 10.1158/1541-7786.MCR-19-0197

strong evidence for development of small molecules targeting USP3 into clinical agents.

Snail is an important EMT-inducing transcription factor and is closely correlated with invasion and metastasis in diverse solid tumors (27–30). Snail is a liable protein and degraded by ubiquitin–proteasome system. Although several E3 ubiquitin ligases for Snail degradation have been identified (31–33), the DUBs for the stabilization of Snail remain less defined. In this study, we identified USP3 serves as a *bona fide* DUB mediating Snail stabilization. Importantly, we found that the loss of tumorigenic capacity caused by USP3 depletion could be largely rescued by ectopic expression of Snail, thus revealing an important role of USP3/Snail signaling axis in mediating the invasive and tumorigenic properties of GBM cells. Future studies are required to elucidate whether other DUBs synergy with USP3 to regulate Snail in human cancers.

In summary, our finding uncovers USP3-mediated Snail stabilization as an important mechanism underlying GBM invasion and progression. Targeting USP3/Snail axis may provide a new promising treatment regimen for GBMs.

Disclosure of Potential Conflicts of Interest

No potential conflicts of interest were disclosed.

Authors' Contributions

Conception and design: L. Fan, Z. Chen, H. Wang, N. Liu
Development of methodology: L. Fan, Z. Chen, N. Liu
Acquisition of data (provided animals, acquired and managed patients, provided facilities, etc.): L. Fan, Z. Chen, X. Wu, X. Cai, S. Feng, J. Lu
Analysis and interpretation of data (e.g., statistical analysis, biostatistics, computational analysis): L. Fan, X. Wu, X. Cai, S. Feng, J. Lu, H. Wang, N. Liu
Writing, review, and/or revision of the manuscript: H. Wang, N. Liu
Administrative, technical, or material support (i.e., reporting or organizing data, constructing databases): L. Fan, Z. Chen, N. Liu
Study supervision: L. Fan, Z. Chen, H. Wang, N. Liu

Acknowledgments

This work was supported by the National Natural Science Foundation of China (81772681, 81670153, and 81872058), the Natural Science Foundation of Jiangsu Province (BK20160098), the Program for Development of Innovative Research Team in the First Affiliated Hospital of NJMU, and the Priority Academic Program Development of Jiangsu Higher Education Institutions.

The costs of publication of this article were defrayed in part by the payment of page charges. This article must therefore be hereby marked *advertisement* in accordance with 18 U.S.C. Section 1734 solely to indicate this fact.

Received February 18, 2019; revised May 14, 2019; accepted June 21, 2019; published first July 2, 2019.

References

1. Behin A, Hoang-Xuan K, Carpentier AF, Delattre JY. Primary brain tumours in adults. Lancet 2003;361:323–31.
2. Furnari FB, Fenton T, Bachoo RM, Mukasa A, Stommel JM, Stegh A, et al. Malignant astrocytic glioma: genetics, biology, and paths to treatment. Genes Dev 2007;21:2683–710.
3. Ostrom QT, Gittleman H, Liao P, Rouse C, Chen Y, Dowling J, et al. CBTRUS statistical report: primary brain and central nervous system tumors diagnosed in the United States in 2007–2011. Neuro Oncol 2014;16:iv1–63.
4. Tanaka S, Louis DN, Curry WT, Batchelor TT, Dietrich J. Diagnostic and therapeutic avenues for glioblastoma: no longer a dead end? Nat Rev Clin Oncol 2013;10:14–26.
5. Stupp R, Hegi ME, Mason WP, van den Bent MJ, Taphoorn MJ, Janzer RC, et al. Effects of radiotherapy with concomitant and adjuvant temozolomide versus radiotherapy alone on survival in glioblastoma in a randomised phase III study: 5-year analysis of the EORTC-NCIC trial. Lancet Oncol 2009;10:459–66.
6. Carlsson SK, Brothers SP, Wahlestedt C. Emerging treatment strategies for glioblastoma multiforme. EMBO Mol Med 2014;6:1359–70.
7. Giese A, Bjerkvig R, Berens ME, Westphal M. Cost of migration: invasion of malignant gliomas and implications for treatment. J Clin Oncol 2003;21:1624–36.
8. Thiery JP, Acloque H, Huang RY, Nieto MA. Epithelial-mesenchymal transitions in development and disease. Cell 2009;139:871–90.
9. Lamouille S, Xu J, Derynck R. Molecular mechanisms of epithelial-mesenchymal transition. Nat Rev Mol Cell Biol 2014;15:178–96.
10. De Craene B, Berx G. Regulatory networks defining EMT during cancer initiation and progression. Nat Rev Cancer 2013;13:97–110.
11. Peinado H, Olmeda D, Cano A. Snail, Zeb and bHLH factors in tumour progression: an alliance against the epithelial phenotype? Nat Rev Cancer 2007;7:415–28.
12. Komander D, Clague MJ, Urbe S. Breaking the chains: structure and function of the deubiquitinases. Nat Rev Mol Cell Biol 2009;10:550–63.
13. Cheng YC, Shieh SY. Deubiquitinating enzyme USP3 controls CHK1 chromatin association and activation. Proc Natl Acad Sci U S A 2018;115:5546–51.
14. Fu S, Shao S, Wang L, Liu H, Hou H, Wang Y, et al. USP3 stabilizes p53 protein through its deubiquitinase activity. Biochem Biophys Res Commun 2017;492:178–83.
15. Cui J, Song Y, Li Y, Zhu Q, Tan P, Qin Y, et al. USP3 inhibits type I interferon signaling by deubiquitinating RIG-I-like receptors. Cell Res 2014;24:400–16.
16. Sharma N, Zhu Q, Wani G, He J, Wang QE, Wani AA. USP3 counteracts RNF168 via deubiquitinating H2A and gammaH2AX at lysine 13 and 15. Cell Cycle 2014;13:106–14.
17. Fang CL, Lin CC, Chen HK, Hseu YC, Hung ST, Sun DP, et al. Ubiquitin-specific protease 3 overexpression promotes gastric carcinogenesis and is predictive of poor patient prognosis. Cancer Sci 2018;109:3438–49.
18. Wang H, Wu W, Wang HW, Wang S, Chen Y, Zhang X, et al. Analysis of specialized DNA polymerases expression in human gliomas: association with prognostic significance. Neuro Oncol 2010;12:679–86.
19. Zhang R, Luo H, Wang S, Chen Z, Hua L, Wang HW, et al. MiR-622 suppresses proliferation, invasion and migration by directly targeting activating transcription factor 2 in glioma cells. J Neurooncol 2015;121:63–72.
20. Zheng H, Shen M, Zha YL, Li W, Wei Y, Blanco MA, et al. PKD1 phosphorylation-dependent degradation of SNAIL by SCF-FBXO11 regulates epithelial-mesenchymal transition and metastasis. Cancer Cell 2014;26:358–73.
21. Zhou BP, Deng J, Xia W, Xu J, Li YM, Gunduz M, et al. Dual regulation of Snail by GSK-3beta-mediated phosphorylation in control of epithelial-mesenchymal transition. Nat Cell Biol 2004;6:931–40.
22. Aiello NM, Kang Y. Context-dependent EMT programs in cancer metastasis. J Exp Med 2019;216:1016–26.
23. Jiang S, Wang X, Song D, Liu X, Gu Y, Xu Z, et al. Cholesterol induces epithelial-to-mesenchymal transition of prostate cancer cells by suppressing degradation of EGFR through APMAP. Cancer Res 2019;79:3063–75.
24. Xu Y, Xu H, Li M, Wu H, Guo Y, Chen J, et al. KIAA1199 promotes sorafenib tolerance and the metastasis of hepatocellular carcinoma by activating the EGF/EGFR-dependent epithelial-mesenchymal transition program. Cancer Lett 2019;454:78–89.
25. Kröger C, Afeyan A, Mraz J, Eaton EN, Reinhardt F, Khodor YL, et al. Acquisition of a hybrid E/M state is essential for tumorigenicity of basal breast cancer cells. Proc Natl Acad Sci U S A 2019;116:7353–62.
26. Wang Z, Yang J, Di J, Cui M, Xing J, Wu F, et al. Downregulated USP3 mRNA functions as a competitive endogenous RNA of SMAD4 by

Published OnlineFirst July 2, 2019; DOI: 10.1158/1541-7786.MCR-19-0197

sponging miR-224 and promotes metastasis in colorectal cancer. Sci Rep 2017;7:4281.
27. Peng B, Ortega J,Gu L, Chang Z, Li GM. Phosphorylation of proliferating cell nuclear antigen promotes cancer progression by activating the ATM/Akt/GSK3beta/Snail signaling pathway. J Biol Chem 2019;294:7037–45.
28. Jung HY, Fattet L, Tsai JH, Kajimoto T, Chang Q, Newton AC, et al. Apical-basal polarity inhibits epithelial-mesenchymal transition and tumour metastasis by PAR-complex-mediated SNAI1 degradation. Nat Cell Biol 2019;21:359–71.
29. Zhao GX, Xu YY, Weng SQ, Zhang S, Chen Y, Shen XZ, et al. CAPS1 promotes colorectal cancer metastasis via Snail mediated epithelial mesenchymal transformation. Oncogene 2019;38:4574–89.
30. Zhou Y, Lu L, Jiang G, Chen Z, Li J, An P, et al. Targeting CDK7 increases the stability of Snail to promote the dissemination of colorectal cancer. Cell Death Differ 2019;26:1442–52.
31. Sun R, Xie HY, Qian JX, Huang YN, Yang F, Zhang FL, et al. FBXO22 possesses both protumorigenic and antimetastatic roles in breast cancer progression. Cancer Res 2018;78:5274–86.
32. Zhang Y, Zhang X, Ye M, Jing P, Xiong J, Han Z, et al. FBW7 loss promotes epithelial-to-mesenchymal transition in non-small cell lung cancer through the stabilization of Snail protein. Cancer Lett 2018;419:75–83.
33. Liu Y, Zhou H, Zhu R, Ding F, Li Y, Cao X, et al. SPSB3 targets SNAIL for degradation in GSK-3beta phosphorylation-dependent manner and regulates metastasis. Oncogene 2018;37:768–76.

AACR American Association for Cancer Research

Molecular Cancer Research

Ubiquitin-Specific Protease 3 Promotes Glioblastoma Cell Invasion and Epithelial–Mesenchymal Transition via Stabilizing Snail

Ligang Fan, Zhengxin Chen, Xiaoting Wu, et al.

Mol Cancer Res Published OnlineFirst July 2, 2019.